American Mineralogist, Volume 91, pages 1927–1931, 2006

Hydroxylellestadite from Cioclovina Cave (Romania): Microanalytical, structural, and vibrational spectroscopy data

BOGDAN P. ONAC,[1,2,*] HERTA EFFENBERGER,[3] KARL ETTINGER,[4] AND SIMONA CINTA PANZARU[5]

[1]Department of Geology, University of South Florida, 4202 E. Fowler Avenue, SCA 528, Tampa, Florida 33620-6250, U.S.A.
[2]Department of Mineralogy, Babeş-Bolyai University/Speleological Institute, Clinicilor 5, 400006 Cluj, Romania
[3]Institute of Mineralogy and Crystallography, University of Wien, Geozentrum, Althanstraße 14, A-1090 Wien, Austria
[4]Institute of Mineralogy and Petrology, Karl-Franzens University, Universitätsplatz 2, A-8010 Graz, Austria
[5]Department of Molecular Spectroscopy, Babeş-Bolyai University, Kogălniceanu 1, 400084, Cluj, Romania

ABSTRACT

Electron-microprobe analyses of hydroxylellestadite from the Cioclovina Cave (Romania) gave the composition $Ca_{10.27}[(SiO_4)_{2.53}(SO_4)_{2.17}(PO_4)_{1.27}]_{\Sigma=5.97}[(OH)_{1.66}F_{0.21}Cl_{0.16}]_{\Sigma=2.03}$. The mineral is translucent to transparent, light orange, slightly fluorescent, has a vitreous luster and <1.5 mm in length. A single-crystal X-ray structure investigation gave the average space-group symmetry $P6_3/m$ [$R1(F) = 0.038$ for 783 reflections up to $2\theta_{MoK\alpha} = 70°$ and 42 variables, $a = 9.496(2)$, $c = 6.920(2)$ Å, $V = 540.4$ Å^3, and $Z = 2$]. Some atoms exhibit large anisotropic displacements. Ordering of atoms along with a symmetry reduction is not verified. Fourier-transformed infrared (FT-IR) and micro-Raman spectra exhibit a distinct contribution from $(PO_4)^{3-}$ modes along with the characteristic $(SO_4)^{2-}$ and $(SiO_4)^{4-}$ modes. The occurrence is quite unusual and suggests that an intense thermal process affected a restricted area within the cave. Hydroxylellestadite is associated with berlinite, another high-temperature mineral. It is likely to have formed within highly phosphatized, silicate-rich, carbonate-mudstone sediments heavily compacted and thermally transformed due to in situ bat guano combustion.

Keywords: Hydroxylellestadite, britholite group, bat guano combustion, cave minerals, Cioclovina Cave, Romania

INTRODUCTION

Substantial deposits of bat guano are found primarily in caves situated in temperate and tropical regions. Fresh guano is a mixture of nitrogenous organic compounds and moderate to high amounts of phosphate (Hill and Forti 1997). The mineralogy of guano-related compounds is complex. Over 60 secondary cave minerals are precipitated when guano-leached solutions, rich in N and P, react with the carbonate bedrock or clay sediments. Typical low-temperature phosphate minerals found in the cave environment include brushite, ardealite, taranakite, and members of the apatite group. Hydroxylapatite and carbonate-hydroxylapatite are the most thermodynamically stable under ordinary cave conditions (Onac 2004). Less commonly, spontaneous combustion of guano is responsible for the generation of high-temperature phosphates (Martini 1994a; Onac and White 2003) or compounds with an apatite-type structure such as hydroxylellestadite, a mineral of the britholite subgroup.

Natural hydroxylellestadite occurrences have been reported from pegmatite veins (Schnorrer-Köhler and Rewitzer 1991), skarn and pyrometamorphic deposits (McConnell 1937; Harada et al. 1971; Favreau et al. 2004), and from mine dumps (Witzke and Rüger 1998; Sejkora et al. 1999).

Synthetic analogs are known as "technical products," such as burning of industrial waste and cement kilns. Their complex chemical compositions and wide ionic substitutions have motivated an increasing number of studies (von Lampe et al. 1989; Neubauer and Pöllmann 1995; Jegou Saint-Jean and Hansen 2005). An extensive substitution is observed in the silicate-sulfate apatite series according to the general formula $Ca_{10}(SiO_4)_{3-x}(SO_4)_{3-x}(PO_4)_{2x}(OH,F,Cl)_2$, where $x < 3/2$; this causes $\Sigma(Si,S) > P$. It should be noted that all analyses reported in the literature have Si:S ~1:1, which is required for charge balance assuming full occupancy of all atomic sites (e.g., Rouse and Dunn 1982; Sejkora et al. 1999).

Herein we report new chemical, single-crystal X-ray diffraction, FT-IR, and Raman vibrational spectroscopic data of hydroxylellestadite from Cioclovina Cave, Romania.

OCCURRENCE, PHYSICAL, AND OPTICAL PROPERTIES

Cioclovina Cave is located on the southwestern side of the Şureanu Mountains, Romania (longitude 23° 8' 18" E, latitude 45° 34' 28" N) and has developed in Lower Cretaceous-aged limestone. It is renowned for its enormous amount of phosphate-rich sediments that almost entirely filled some 450 m of cave passages (the thickness of sediments varies between 3 and 20 m). By 1941, as much as 30 000 m^3 had been mined out and used as fertilizer providing good exposures of the sediment sequence and allowing for detailed mineralogical work. The origin of phosphate-rich sediments is related to large deposits of bat guano

* E-mail: bonac@cas.usf.edu

and thousands of cave bear remains.

Successive cave flooding events resulted in the accumulation of large quantities of clay and sand that were interbedded with bat guano horizons or completely buried the organic sediment. In some parts of the cave, the weight of the overlying sediments was significant and the underlying material was heavily compacted so that textures and structures of the original sediments no longer can be recognized. Owing to microbial processes, the temperature inside the buried guano increased until spontaneous ignition led to its combustion, converting the sediment to a dark-brown color. The temperature difference between the inner and outer part of the compacted sediments caused cracks to appear. All these thermally induced changes further obliterated the outlines of the original depositional features. Due to these geological conditions, 15 phosphate minerals—including a few very rare species—were discovered (Onac et al. 2002, 2005 and references therein). Cioclovina Cave is the type locality for ardealite (Schadler 1932).

The hydroxylellestadite-bearing sediment occurs only in a dead-end, side passage of the cave and shows the entire above-mentioned thermal transformation features. From the same location and sediment type, the high-temperature phosphate, berlinite has been described (Onac and White 2003).

Re-investigation of chlorellestadite sample (pinkish crust of densely intergrown aggregates) collected and described from Cioclovina Cave (Onac et al. 2002), revealed light-orange aggregates of hydroxylellestadite associated with quartz. XRD confirmed the presence of quartz not the other polymorphs. The aggregate grain size up to 1.5 mm in length and 0.3 mm across were observed. Physical data of the Cioclovina hydroxylellestadite agree well with those given by Harada et al. (1971): the samples have a vitreous luster; they are translucent to transparent; the hardness VHN_{50} (measured with a Vickers micro-hardness tester) is 590(30) kg/mm^2 corresponding to ~4½ on the Mohs' scale; the fracture is irregular, the cleavage is indistinct, the refractive indices (determined using Cargille immersion liquids, λ = 5893 Å, 25 °C) are η_ω = 1.653(2), η_ε = 1.649(2); and the optical character is uniaxial (–). Hydroxylellestadite shows faded white-yellow fluorescence when irradiated with UV light, independent of the excitation frequency. The mineral forms aggregates of xenomorphic crystals.

Analytical methods

A fragment of the pinkish crust was embedded in epoxy resin and polished for back-scattered electron imaging. The chemical analyses were performed in energy- and wavelength-dispersive mode using a Jeol JSM-6310 instrument (University of Graz) with attached EDX Oxford Link Isis and Microspec WDX (analytical conditions: 15 kV, 5 and 10 nA, 1.5–3 µm beam size, WDX: peak count-time 20 s, background count-time 10 s). A 100-s real-time scan in EDS mode revealed F, Si, P, S, Cl, and Ca. No other elements with *Z* greater than 8 were found. The φ-ρ-*Z* program incorporated in the ISIS software was used for data reduction. Apatite (Ca, F), quartz (Si), xenotime (P), celestine (S), and atacamite (Cl) served as standards. The variations of F and Cl X-ray intensities due to anisotropic diffusion in apatite reported by Stormer et al. (1993) were not observed in our samples. The tests we performed showed relatively constant F and Cl count rates over a 150 s time-period, and therefore, we believe that diffusion did not significantly affect our analytical results.

A small crystal chip of hydroxylellestadite from the Cioclovina Cave was examined at the University of Wien with a Nonius Kappa-CCD four-circle diffractometer equipped with a 300 µm diameter capillary-optics collimator (graphite-monochromatized Mo*K*α radiation). Data were corrected for background, Lorentz and polarization effects, and absorption (multi-scan method). Programs used include COLLECT (Nonius 1999), DENZO-SMN (Otwinowski and Minor 1997), and SHELXL-97 (Sheldrick 1997). Experimental details relative to data collection are reported in Table 1.

The FT-IR spectra of hydroxylellestadite (KBr pellet) from Cioclovina Cave were recorded at room temperature using a Bruker Equinox 55 spectrometer (InGaAs detector at the Babeş-Bolyai University in Cluj). Two hundred scans were accumulated. The spectral resolution was 4 cm^{-1}. Micro-Raman spectra of two different samples were taken with a Dilor Labram spectrometer (514.5 nm excitation line) from a 100 mW Spectra Physics Argon ion laser (back-scattering geometry) at the University of Wuerzburg, Germany. The laser excitation was coupled to an optical microscope Olympus U-CMAD-2 with two objectives: DPLAN 20 160/0.17 and ULWD MS-PLAN 80/0.75. In both cases the spectral resolution was 2 cm^{-1} and the acquisition time was 5 × 50 s for each window.

Results

Chemical composition

The composition of hydroxylellestadite is quite homogeneous, both within a given crystal as well as between different samples. The mean of eight analyses on two hydroxylellestadite grains within one polished section yields the empirical formula $Ca_{10.27}[(SiO_4)_{2.53}(SO_4)_{2.17}(PO_4)_{1.27}]_{\Sigma=5.97}[(OH)_{1.66}F_{0.21}Cl_{0.16}]_{\Sigma=2.03}$ (normalized on the basis of 25 O atoms; see Table 2). The strong depletion in Cl and F counterbalanced by enrichment of OH shifts the anion composition to a nearly pure end-member hydroxylellestadite. None of the other members (i.e., F- or Cl-rich ellestadite) was observed in our samples. Water was not determined by analysis but recalculated for charge balance of the chemical formula. A micro-chemical test for carbonate by evaporating CO_2 was negative.

The presence of a large S component (16.85 wt% SO_3), coupled with excess Si (14.73 wt% SiO_2) not balanced by the $(CO_3)^{2-}$ or (Y + REE) and deficiency in P, implies the existence of the charge-compensating substitution $2P^{5+} \leftrightarrow Si^{4+} + S^{6+}$, as proposed by McConnell (1937).

X-ray data collection, space-group determination, and structure refinement

Neutral-atomic complex scattering functions (Wilson 1992) were used; mixed occupancies at the X site (Si:S:P = 2:2:1) and at the *Z* site (O:F:Cl = 1.70:0.15:0.15) were assumed according to the chemical composition found by electron-microprobe

Table 1. Single-crystal X-ray data collection and structure refinement for hydroxylellestadite

a (Å), *c* (Å); *V* (Å^3); space group	9.496(2), 6.920(2); 540.4; *P*6$_3$/*m*
Z	2 {$Ca_5[(Si,P,S)O_4]_3(OH,F,Cl)$}
Crystal diameter (mm^3); µ (mm^{-1})	0.045 × 0.050 × 0.065; 3.0
Δφ at 12 distinct ω values (°);	2
collection time (s/°)	110
$2\theta_{max}$ (°); images; crystal-detector	70; 723
distance (mm)	30
Data collection temperature (K)	293
Measured reflections	9429
$R_{int} = \Sigma\lvert F_o^2 - F_o^2(\text{mean})\rvert/\Sigma F_o^2$	0.043
Unique (n) reflections;*R*1(*F*); *wR*2(F^2)	845; 0.041; 0.090
"Observed" reflections $F_o > 4\sigma(F_o)$; *R*1(*F*)	783; 0.038
GooF = $\{\Sigma[w(F_o^2 - F_c^2)^2]/(n - p)\}^{0.5}$	1.059
Variable parameters (p)	42
Δ/σ; $\Delta\rho_{min}$, $\Delta\rho_{max}$ (e/Å^3)	<0.001; –1.33, 1.77
Extinction coefficient	0.012(3)

Notes: $R1(F) = \Sigma(\lVert F_o\rvert - \lvert F_c\rVert)/\Sigma F_o$; $wR2(F^2) = [\Sigma w(F_o^2 - F_c^2)^2/\Sigma wF_o^4]^{1/2}$; $w = 1/[\sigma^2(F_o^2) + (0.033*P)^2 + (1.37*P)]$, $P = [\max(0,F_o^2)] + 2*F_c^2)/3]$.

TABLE 2. Electron-microprobe analyses of hydroxylellestadite from Cioclovina Cave

Wt%	Mean of 8 analyses	Range	Number of ions*	
SiO_2	14.73	14.54–14.94	Si	2.53
P_2O_5	8.73	8.45–8.92	P	1.27
SO_3	16.85	16.53–17.09	S	2.17
CaO	55.84	54.92–56.93	Ca	10.27
F	0.39	0.36–0.43	F	0.21
Cl	0.54	0.49–0.56	Cl	0.16
H_2O	1.45	–	–	–
OH	–	–	–	1.90
–O = (F,Cl)	0.29	–	–	–
Total	98.24	–	–	–

* Based on 25 O atoms (anhydrous).

analyses. Any trials to refine the scattering power at the A, X, or Z sites did not differ significantly from that assumption and made the refinement unstable; therefore during the final refinement the occupancy factors were not allowed to vary.

The parental structure of the apatite-type compounds (space-group symmetry $P6_3/m$) is characterized by two crystallographically different positions for the A atoms and one each for the X and Z atoms. The chemical composition indicates some tetrahedral substitution for $(SiO_4)^{4-} + (SO_4)^{2-} \leftrightarrow 2(PO_4)^{3-}$. The ionic radius of Si^{4+} (0.26 Å) is large compared to that of P^{5+} (0.17 Å) and S^{6+} (0.12 Å), (Shannon 1976) so the size of the XO_4 tetrahedra are significantly different. Also the F and Cl anions as well as the hydroxyl group differ in their space requirements. The symmetry reduction from hexagonal has been discussed repeatedly for partly Si-substituted apatites (McConnell 1938; Sudarsanan 1980; Rouse and Dunn 1982; Hughes and Drexler 1991; Organova et al. 1994; Neubauer and Pöllmann 1995; Jegou Saint-Jean and Hansen 2005).

As expected from the investigations reported in literature, the refinement in space group $P6_3/m$ showed significant anisotropic displacement parameters. Most affected were the atoms at the Ca2, O3, and Z sites. In addition, the difference Fourier summations exhibited large electron densities in the vicinity of Ca2 (2.08 eÅ^{-3}) and O3 (1.09 eÅ^{-3}). The X-O bond distances of 1.547(2), 2×, 1.547(2) and 1.550(2) Å are in agreement with X = (Si,S,P).

The full reciprocal sphere was measured to enable refinements in all subgroups of the space group $P6_3/m$: $P6_3$, $P\bar{3}$, $P\bar{6}$,$P3$, $P112_1/m$, $P11m$, $P112_1$, $P\bar{1}$, and $P1$. No streaks or (weak) superstructure reflections were seen. The release of symmetry elements would allow different sites for Si and (P, S) atoms. Furthermore, Z atoms (F, O_h, and Cl) may be located at individual sites along the direction [00z]. Ordering of these atoms caused by the requirements of their individual crystal-chemical behavior seemed possible at the beginning. However, none of the refinements based on lower symmetries yielded a model exhibiting at least partly ordered SiO_4 and [(S,P)O_4] tetrahedra or Cl, O_h, and F atoms; the correlation-matrix elements for symmetry-related parameters in the $P6_3/m$ model were always above 0.90. Despite some reductions of R values, the refined models were not significant. The standard deviations for some of the Ca-O and X-O bond distances were above 0.01 Å. The results were improved by considering multiple twinning along the former 6_3 axis during refinements in triclinic and monoclinic space groups. Depending on the refined model, the three twin components were calculated between 0.15 and 0.70.

The lowest R values [$wR2 = 0.064$ for 845 data points and 56 variables, $R1 = 0.026$ for 783 reflections with $F_o > 4\sigma(F_o)$] were obtained for split sites of the atoms Ca2 and O3, which maintain the parental symmetry of $P6_3/m$. However, the standard deviation of ~0.012 Å and the correlation matrix elements of ~0.95 showed that the collected data set did not justify splitting these atom sites. As a conclusion, the crystal used for structure investigation did not allow any refinement in a space group with lower symmetry; the symmetry of hydroxylellestadite from Cioclovina Cave is, on average, $P6_3/m$. The best approximation to the symmetry was obtained for the refinement in the $P6_3/m$ space-group and allowing only anisotropic displacement parameters for all atom sites. Structural parameters and bond distances are listed in Tables 3 and 4, respectively.

The refinement of hydroxylellestadite from the Chichibu mine, Japan (Sudarsanan 1980) was performed in space group $P2_1/m$. That sample exhibits an Si:S ratio of ~1:1 and very low P content. The standard deviations of the atomic coordinates are moderate with the exception of some of the split A sites. For chlorellestadite (Jegou Saint-Jean and Hansen 2005) and fluorellestadite (Pajares et al. 2002), structure refinements in space group $P6_3/m$ were reported. The most significant differences were observed for the position (0 0 z) of the Z atoms: z = 0.451(2) in chlorellestadite and 0.250 in fluorellestadite. In the $P2_1/m$ structure of hydroxylellestadite, Sudarsanan (1980) refined separate sites for O_h: $z = 0.2023(5)$, F: $z = 0.250$, and Cl: $z = 0.3644(5)$. During the present refinement, Z is on a half-occupied position (0 0 z) with $z = 0.1975(9)$; the principal mean square atomic displacements are 0.070 Å^2 parallel and 0.017 Å^2 perpendicular to the 6_3 axis, respectively, which agrees with

TABLE 4. Bond distances (Å) for hydroxylellestadite

X-O1	1.547(2)	Ca2-O3	2.3628(18), 2x
X-O3	1.547(2), 2×	Ca2-O2	2.3765(24)
X-O2	1.550(2)	Ca2-Z	2.3931(13), 2x
		Ca2-O3	2.5369(20), 2x
Ca1-O1	2.4169(17), 3×	Ca2-O1	2.726(2)
Ca1-O2	2.4746(18), 3×		
Ca1-O3	2.8053(23), 3×	Z···Z	2.738(13)

TABLE 3. Fractional atomic coordinates and displacement parameters for hydroxylellestadite

	Wyckoff notation	site occupation	x	y	z	U_{11}	U_{22}	U_{33}	U_{23}	U_{13}	U_{12}	U_{equiv}
X = (Si,P,S)	6(*h*)	1.0	0.39939(8)	0.37013(8)	¼	0.0147(3)	0.0133(3)	0.0120(3)	0	0	0.0077(2)	0.01300(15)
Ca1	4(*f*)	1.0	½	½	0.00183(11)	0.0372(3)	= U_{11}	0.0123(3)	0	0	= ½ U_{11}	0.02887(20)
Ca2	6(*h*)	1.0	0.24567(8)	–0.00670(8)	¼	0.0276(3)	0.0281(3)	0.0173(3)	0	0	0.0138(2)	0.02440(17)
O1	6(*h*)	1.0	0.3276(3)	0.4848(3)	¼	0.0359(12)	0.0244(10)	0.0208(9)	0	0	0.0201(9)	0.0248(4)
O2	6(*h*)	1.0	0.5879(3)	0.4659(3)	¼	0.0186(9)	0.0193(9)	0.0387(13)	0	0	0.0077(8)	0.0263(5)
O3	12(*i*)	1.0	0.3460(3)	0.2592(2)	0.0696(3)	0.0521(11)	0.0305(8)	0.0244(8)	–0.0070(7)	–0.0166(8)	0.0271(8)	0.0328(4)
Z = (O_h,F,Cl)	4(*e*)	0.5	0	0	0.1975(9)	0.0170(9)	= U_{11}	0.070(6)	0	0	= ½ U_{11}	0.0347(19)

Note: The anisotropic displacement parameters are defined as: $\exp[-2\pi^2 \Sigma_{i=1}^{3} \Sigma_{j=1}^{3} U_{ij} a^*_i a^*_j h_i h_j]$, U_{eq} according to Fischer and Tillmanns (1988).

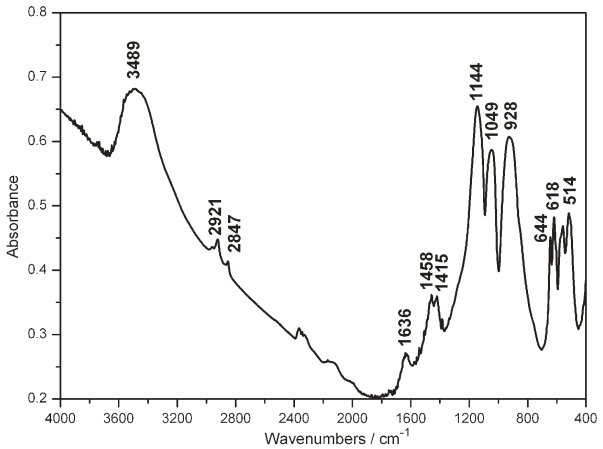

FIGURE 1. FT-IR spectrum.

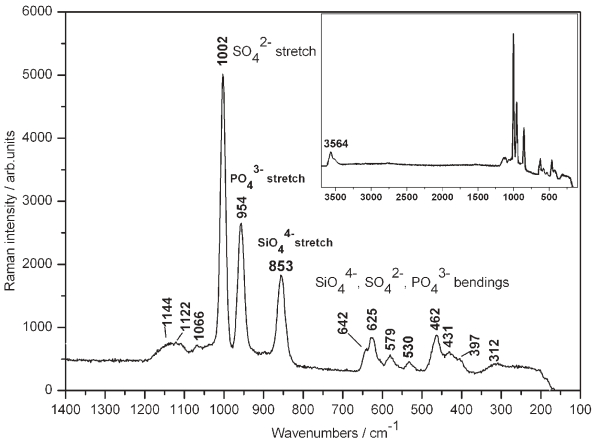

FIGURE 2. Micro-Raman spectrum. The inset shows an enlarged view of the 3500 cm^{-1} region of hydroxylellestadite spectrum.

the dominant occupancy of hydroxyl groups and only minor substitutions by F and Cl atoms.

Vibrational spectroscopy

The FT-IR spectrum (Fig. 1) displays a broad band centered at 3489 cm^{-1} that was assigned to OH-stretching mode corresponding to an O-H···O distance of about 2.88 Å (Libowitzky 1999). This value is larger than the one found from the crystal-structure refinement [2.738(13) Å], but it is affected by large displacements of the O atoms. In contrast, Sejkora et al. (1999) found seven absorption lines in their Cl-enriched hydroxylellestadite. Harada et al. (1971) also described one band, at 3600 cm^{-1}, for a specimen from Chichibu. Sudarsanan (1980) mentioned the decrease of the IR oscillator strength for OH groups in the case where Cl atoms act as acceptors for the H bond; the influence of F atoms is less significant.

The weak IR absorption bands at 2921 and 2847 cm^{-1} are related to C-H stretching modes. We interpret the bands at 1458 and 1415 cm^{-1} as C-H bending modes from organic impurities (sample preparation) as opposed to the CO_3^{2-} group suggested by Arkhipenko and Moroz (1997) as the micro-chemical test for carbonate was negative.

The large band centered at 928 cm^{-1} with a shoulder at 853 cm^{-1} is characteristic of the SiO_4^{4-} group. However, the shifts observed between our vibrational frequencies and those reported by Harada et al. (1971), Arkhipenko and Moroz (1997), and Socrates (2001) reflect the partial substitution of $(SiO_4)^{4-}$ and $(SO_4)^{2-}$ for the $(PO_4)^{3-}$ group in the apatite structure. Based on Santos and Clayton (1995) and Popović et al. (2005), the IR bands at 1144 and 1049 cm^{-1} from our spectrum were assigned to either double- or single-bond stretchings of an orthophosphate and not to the $(SO_4)^{2-}$ group as suggested by Harada et al. (1971) and Sejkora et al. (1999).

The micro-Raman spectrum (Fig. 2) exhibits diagnostic vibrational bands at 3564, 1002, 954, 853, 625, and 462 cm^{-1}. The high-wavenumber region of the spectrum characteristic of OH groups was not reported by Arkhipenko and Moroz (1997), probably due to the increase in intensity of the spectral background that completely covered any OH-stretching bands. Such background was not observed here. Our micro-Raman spectrum reveals the OH-stretching feature at 3564 cm^{-1} (with a shoulder at 3517 cm^{-1}; Fig. 2) that correlates well with the H bond distances of 2.738(13) Å. In the 1400–200 cm^{-1} range, the micro-Raman spectrum exhibits well-resolved bands of silicate, sulfate, and phosphate tetrahedra.

DISCUSSION

Natural hydroxylellestadite occurrences have been documented from pegmatite veins, skarn deposits, and burned mine dumps, but this mineral has never been reported from a cave. Although the occurrences are diverse, all these locations have one feature in common: the mineral formed in high-temperature environments (i.e., above 500 °C). However, the significant difference between the Cioclovina hydroxylellestadite and those from other locations is the distinct enrichment of PO_4 and the complete absence of CO_3.

The single-crystal X-ray structure investigation confirmed the presence of hydroxylellestadite. The occurrence of average $P6_3/m$ symmetry may be an indication that the hydroxylellestadite formed at the border of its stability field or during a relative short time so that the order according to $P2_1/m$ symmetry (Sudarsanan 1980) was not achieved. The overall vibrational analyses of our samples show significant contributions from phosphate modes, characteristic of an apatite with a partial substitution of $(PO_4)^{3-}$ ions by $(SO_4)^{2-}$ and $(SiO_4)^{4-}$. The most obvious difference when compared to the previously reported data is the increasing relative intensity of the $(PO_4)^{3-}$ lines.

To form hydroxylellestadite in a cave, two requirements need to be satisfied: the chemical ingredients and the heating source. Several minerals that are known to occur in Cioclovina Cave could have acted as starting material. The large number of phosphate minerals (e.g., ardealite, brushite, carbonate-hydroxylapatite, crandallite, fluorapatite, monetite, etc.) derived from the bat guano explains our PO_4-rich hydroxylellestadite. The sulfate likely originated from gypsum and/or ardealite (both minerals are abundant in this cave), whereas silica is thought to be contributed by the clastic sediments (sand and clay) that covered the guano deposits. Calcium comes from limestone, secondary cave calcite deposits or any of the Ca-phosphates. Either a Ca-phosphate like apatite (in the presence of sulfate and silica) or a mixture of the above ingredients could have been transformed

into hydroxylellestadite if spontaneous combustion of bat guano occurred locally within the cave.

Documenting the existence of this rare, high-temperature mineral within Cioclovina Cave, our study lends significant support to a local, intense thermal process that affected a phosphatized, silicate-rich carbonate-mudstone sequence occurring in a restricted area within the cave. This scenario was suggested by Onac and White (2003) when addressing the genesis of berlinite, but questioned by Marincea and Dumitraş (2005). Considering that bat guano combustion is a poorly known process (Martini 1994b; Forti 2005), further systematic investigations combining mineralogical, geochemical, and spectroscopic techniques are needed gain better understanding of this particular genetic mechanism within the unique environment represented by Cioclovina Cave.

ACKNOWLEDGMENTS

This work would not have been possible without the enthusiasm of R. Breban, who brought to our attention the unusual mineral assemblage from Cioclovina Cave. The Romanian Commission of Nature Protection is thanked for granting permission to collect additional samples for the present study. Thanks are due to E. Libowitzky for many insightful discussions on the significance of FT-IR and FT-Raman spectra. The manuscript was improved thorough the suggestions of reviewers R. Thompson, F. Camara, and Laurence Garvie who served as Associate Editor. J. Harden and L. Florea improved the English of the manuscript. Type material is deposited in the Mineralogical Museum of the "Babeş-Bolyai" University in Cluj, Romania. This study was supported by a Romanian CNCSIS grant (no. 53/1696) to B.P.O.

REFERENCES CITED

Arkhipenko, D.K. and Moroz, T.N. (1997) Vibrational spectrum of natural ellestadite. Crystallography Reports, 42, 651–656.

Favreau, G., Meisser, N., and Chiappero, P.J. (2004) Saint-Maime (alpes-de-Haute-Provance): un éxemple de pyormétamorphisme en region provençale. Le Cahier des Micromonteurs, 85, 59–91.

Fischer, R.X. and Tillmanns, E. (1988) The equivalent isotropic displacement factor. Acta Crystallographica, C44, 775–776.

Forti, P. (2005) Genetic processes of cave minerals in volcanic environments: an overview. Journal of Cave and Karst Studies, 67, 3–13.

Harada, K., Nagashima, K., Nakao, K., and Kato, A. (1971) Hydroxylellestadite, a new apatite from Chichibu mine, Saitama prefecture, Japan. American Mineralogist, 56, 1507–1518.

Hill, C.A. and Forti, P. (1997) Cave minerals of the world (2nd edition), 464 p. National Speleological Society, Huntsville, Alabama.

Hughes, J.M. and Drexler, J.W. (1991) Cation substitution in the apatite tetrahedral site: crystal structure of type hydroxylellestadite and type fermorite. Neues Jahrbuch für Mineralogie Monatshefte, 327–336.

Jegou Saint-Jean, S. and Hansen, S. (2005) Nonstoichiometry in chlorellestadite. Solid State Sciences, 7, 97–102.

Libowitzky, E. (1999) Correlation of O-H stretching frequencies and O-H···O hydrogen bond lengths in minerals. Monatshefte für Chemie, 130, 1047–1059.

Marincea, Ş. and Dumitraş, D.-G. (2005) First reported sedimentary occurrence of berlinite ($AlPO_4$) in phosphate-bearing sediments from Cioclovina Cave, Romania—Comment. American Mineralogist, 90, 1203–1208.

Martini, J.E.J. (1994a) Two new minerals originated from bat guano combustion in Arnhem Cave, Namibia. Bulletin of the South African Speleological Association, 33, 66–69.

——— (1994b) The combustion of bat guano - a poorly known phenomenon. Bulletin of the South African Speleological Association, 33, 70–72.

McConnell, D. (1937) The substitution of SiO_4^- and SO_4^- groups for PO_4^- groups in the apatite structure; ellestadite, the end-member. American Mineralogist, 22, 977–986.

——— (1938) A structural investigation of the isomorphism of the apatite group. American Mineralogist, 23, 1–19.

Neubauer, J. and Pöllmann, H. (1995) Solid solution series of silico-sulphate-cholride-apatites. Neues Jahrbuch für Mineralogie Abhandlungen, 168, 237–258.

Nonius, B.V. (1999) "Collect." Data collection software. Brucker AXS, http://www.bruker-axs.de/.

Onac, B.P. (2004) Minerals. In D.C. Culver and W.B. White, Eds., Encyclopedia of caves, p. 371–378. Elsevier/Academic Press, Amsterdam.

Onac, B.P. and White, W.B. (2003) First reported sedimentary occurrence of berlinite ($AlPO_4$) in phosphate-bearing sediments from Cioclovina Cave, Romania. American Mineralogist, 88, 1395–1397.

Onac, B.P., Breban, R., Kearns, J., and Tămaş, T. (2002) Unusual minerals related to phosphate deposits in Cioclovina Cave, Şureanu Mts. (Romania). Theoretical and Applied Karstology, 15, 27–34.

Onac, B.P., Ettinger, K., Kearns, J., and Balasz, I.I. (2005) A modern, guano-related occurrence of foggite, $CaAl(PO_4)(OH)_2 \cdot H_2O$ and churchite-(Y), $YPO_4 \cdot 2H_2O$ in Cioclovina Cave, Romania. Mineralogy and Petrology 85, 291–302.

Organova, N.I., Rastsvetaeva, R.K., Kuz'mina, O.V., Arapova, G.A., Litsarev, M.A., and Fin'ko, V.I. (1994) Crystal structure of low-symmetry ellestadite in comparison with other apatitelike structures. Kristallografiya, 39, 278–282.

Otwinowski, Z. and Minor, W. (1997) Processing of X-ray diffraction data collected in oscillation mode. In C.W. Carter, Jr. and R.M. Sweet, Eds., Methods in Enzymology, 276, p. 307–326. Macromolecular Crystallography A, Academic Press, New York.

Pajares, I., de la Torre, Á.G., Martínez-Ramírez, S., Puertas, F., Blanco-Varela, M.-T., and Aranda, M.A.G. (2002) Quantitative analysis of mineralized white Portland clinkers: the structure of fluorellestadite. Powder Diffraction, 17, 281–286.

Popović, L., de Waal, D., and Boeyens, J.C.A. (2005) Correlation between Raman wavenumbers and P-O bond lengths in crystalline inorganic phosphates. Journal of Raman Spectroscopy, 36, 2–11.

Rouse, R.C. and Dunn, P.J. (1982) A contribution to the crystal chemistry of ellestadite and silicate sulfate apatites. American Mineralogist, 67, 90–96.

Santos, R.V. and Clayton, R.N. (1995) The carbonate content in high temperature apatite: An analytical method applied to apatite from the Jacupiranga alkaline complex. American Mineralogist, 80, 336–344.

Schadler, J. (1932) Ardealite, ein neues Mineral $CaHPO_4\,CaSO_4.4H_2O$. Zentralblatt für Mineralogie, A, 40–41.

Schnorrer-Köhler, G. and Rewitzer, C. (1991) Bendada—a phosphate pegmatite in the middle part of Portugal. Lapis, 16, 21–33.

Sejkora, J., Houzar, S., and Šrein, V. (1999) Cl-rich hydroxylellestadite from Zastávka near Brno. Acta Musei Moraviae, Scientiae Geologicae, 84, 49–59 (in Czech with English abstract).

Shannon, R.D. (1976) Revised effective ionic radii and systematic studies of interatomic distances in halides and chalcogenides. Acta Crystallographica, A32, 751–767.

Sheldrick, G.M. (1997) SHELXL-97, a program for crystal structure refinement. University of Göttingen, Germany.

Socrates, G. (2001) Infrared and Raman Characteristic Group Frequencies, Tables and Charts. Wiley, Chichester.

Stormer, J.C., Jr., Pierson, M.L., and Tacker, R.C. (1993) Variation of F and Cl X-ray intensity due to anisotropic diffusion in apatite during electron microprobe analysis. American Mineralogist, 78, 641–648.

Sudarsanan, K. (1980) Structure of hydroxylellestadite. Acta Crystallographica, B36, 1636–1639.

von Lampe, F., Grimmer, A.-R., and Wallis, B. (1989) Preparation and characterization of the calcium silicate sulfate chloride $Ca_4(SiO_4)(SO_4)Cl_2$. Cement and Concrete Research, 19, 595–602.

Wilson, A.J.C., Ed. (1992) International tables for crystallography. Vol. C, Mathematical, physical and chemical tables, 883 p. Kluwer Academic Publishers, Dordrecht.

Witzke, T. and Rüger, F. (1998) Die Minerale der Ronneburger und Culmitzscher Lagerstäten in Thüringen. Lapis, 7–8, 26–64.

MANUSCRIPT RECEIVED NOVEMBER 9, 2005
MANUSCRIPT ACCEPTED APRIL 27, 2006
MANUSCRIPT HANDLED BY LAURENCE GARVIE